VALIDATION OF A HUMAN FE LOWER LIMB MODEL FOR A CHILD PEDESTRIAN AGAINST ACCIDENT DATA

Osamu Ito[1], Masayoshi Okamoto[1], Yukou Takahashi[1], Fumie Mori[2], Mark U. Meissner[3], Costin D. Untaroiu[3], Jeff R. Crandall[3]

[1] Honda R&D Co., Ltd. Automobile R&D Center, [2] PSG Co., Ltd.
[3]University of Virginia Center for Applied Biomechanics

ABSTRACT

Due to the lack of sufficient data for children, validation of the impact response of a child dummy or a child finite element (FE) model is a big challenge. This study used multi-body simulations along with optimization techniques for estimating impact conditions of a particular child pedestrian accident case selected from an in-depth pedestrian accident database. FE child model simulations with failure criteria were run using the estimated impact conditions, and the predicted and observed injuries were compared. The results of the comparison showed that the model can predict the lower limb injuries described in the accident data within the estimated bone material property variation.

Key words: Optimization Methods, Accident Analysis, Finite Element Method, Children

THE CURRENT PEDESTRIAN test procedure includes testing for the head and lower limb of adults, while only the head impactor test is applied for children. However, recent studies showed that the lower limb is the most frequently injured body region in severe child pedestrian injuries. Based on this, the authors have developed a FE model for a child pedestrian lower limb to be used as an evaluation tool (Okamoto et al., 2003). In general, material property data for children is very limited primarily due to ethics issues, resulting in difficulties in validating child FE models. In this study, the FE lower limb model for a child pedestrian developed by the authors was validated against a child pedestrian accident case chosen from the Pedestrian Crash Data Study (PCDS) database by the National Highway Traffic Safety Administration (NHTSA).

METHODOLOGY

ACCIDENT DATA

Given that the purpose of this study was to validate a FE lower limb model for a child, a child pedestrian accident case with lower limb fractures was selected from the PCDS database. The accident case summary is provided in Fig. 1. The contact locations between the vehicle and pedestrian are shown in Fig. 2.

ESTIMATION OF IMPACT CONDITIONS

MADYMO was used for estimating impact conditions because of relatively short computational time given the need for multiple runs to optimize impact conditions. A six-year-old child pedestrian model from the MADYMO library was scaled to match the anthropometry of the case pedestrian by referring to the GEBOD anthropometry database. The vehicle model was created by converting an external shape model obtained from the ViewPoint Database to a MADYMO facet model. Due to the

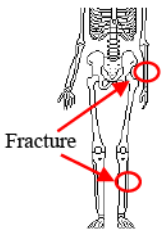

Vehicle Information
Impact Speed：41km/h (estimated)
Contact Location：Hood, Bumper, Windshield

Pedestrian Information
Sex：Female **Age**：9 **Height**：152cm
Weight：27kg
Injuries：left ulna fracture, left tibia fracture, facial abrasions

Fig. 1 Accident summary

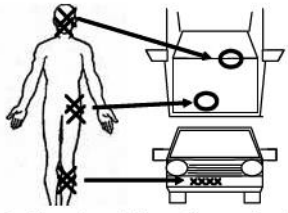

Fig. 2 Contact locations between pedestrian and vehicle

lack of the stiffness characteristics of the case vehicle, the stiffness of a different vehicle with similar front end geometry was used.

Impact condition optimization was performed using a combination of an optimization software (modeFRONTIER) and MADYMO. In order to calculate relative distance, small ellipsoid targets were defined on the models at corresponding locations to the contact points between the vehicle and pedestrian. In the accident case selected for this study, contact marks were identified at the rear end of the hood (presumed as the head contact point) and the leading edge of the hood (presumed as the pelvis contact point). The ellipsoid targets were defined at these locations (Fig. 3). As shown in equation (1), the sum of the relative distances between the corresponding targets on the vehicle and pedestrian models was defined as the objective function, and optimizations were run to minimize this objective function.

Objective function = *Head relative distance + Pelvis relative distance* *(1)*

The vehicle speed, pedestrian speed and pedestrian position (position of the pedestrian relative to the vehicle in the direction of vehicle width) were defined as design variables for optimization. Based on Mizuno (2003), the pedestrian gait cycle was discretized as shown in Fig. 4. The discretized gait stances were not included in the design variables and optimization was performed for the S-4 and S-5 stances in Fig. 4 due to the statement in the accident data that the pedestrian right foot had been off the ground at the time of impact.

INJURY PREDICTION USING FE MODEL

FE Model Set-up

The impact conditions obtained from the optimization were used to set up the FE model, and car-pedestrian impact simulations were run using PAM-CRASH. An upper body model consisting of rigid segments linked by joint elements was integrated into the lower limb FE model developed by the authors based on MRI scans from a six-year-old child (Okamoto et al., 2003) to create a baseline pedestrian model. The joint characteristics of the upper body model were determined by scaling those from an adult pedestrian model developed by Takahashi et al. (2000) using the scaling method described by Langhaar (1951). The baseline model was then scaled to the anthropometry of the case pedestrian. The stance of the model was modified to represent the S-4 and S-5 stances used in the impact condition optimization. Since the femur and tibia were connected using ligament models rather than using a joint element for the knee joint, the shape of the knee ligament models in these stances was defined by running dynamic knee joint bending simulations (Fig. 5). The vehicle model employed in the MADYMO optimization was simply converted to a PAM-CRASH model.

Bone Material Properties

Due to limited data available for children, it was necessary to estimate bone material parameters for a child to simulate child lower limb fractures using a FE model. For the femur and tibia, Ivarsson et al. (2004) estimated the average bone material parameters for human children as a function of age from published dog test results and correlation between human and dog ages. In general, there are significant individual differences in terms of the material property of human bodies. When attempting to predict injuries by reconstructing an accident, it is difficult to determine in advance where the material parameters of the case pedestrian should be positioned within these individual variations. It was therefore necessary to estimate a range of individual variations in material properties for a child to see if observed injuries could be predicted within the upper and lower limits of these variations.

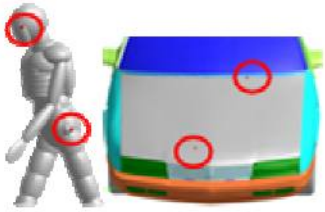

Fig. 3 Target contact points specified on pedestrian and vehicle models

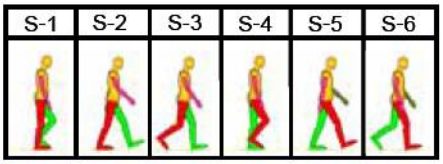

Fig.4 Discretized gait stances

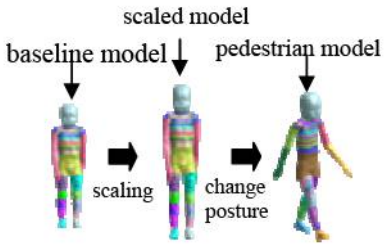

Fig.5 Creation of FE model representing case pedestrian

Since Ivarsson et al. (2004) did not estimate individual variations in material parameters, the ratio of average material properties and their standard deviations determined for adults by Takahashi et al. (2000) was applied to the material properties of children. In addition, the estimated average material properties for children were scaled in such a way that material parameters are consistent with those determined by Takahashi et al. (2000) at age 25 to compensate for the difference between dog and human material properties. Fig. 6 shows the Young's modulus for the femur as a function of age determined for adults by Takahashi et al. along with that for younger population including children estimated by Ivarsson et al. (2004) and modified in this way.

Validation of Bone Material Properties

Using the procedure discussed above, the average and upper and lower limits of the bone stress-strain curve were defined as schematically shown in Fig. 7. The boxes around the yield and failure points represent the range of individual variations in stress and strain at these points. If the injuries sustained in real accidents could be reproduced by any of the stress-strain curves within this range, the hypothesized range of bone material properties could be judged as valid. The confidence level would become higher as the number of cases reproduced increases.

Since there are countless stress-strain curves within the established range, model validation would require an enormous number of simulations. When validating a FE child model against real accidents, only the occurrence or non-occurrence of injury (in this case lower limb bone fracture) is compared. In the present research, the probability of bone fracture was assumed to be determined by the amount of energy that could be absorbed by the bone until failure. Based on this assumption, the stress-strain curves at the maximum and minimum absorbed energy were defined as the upper and lower limits of the range of bone material property variations. The properties between these limits were proportionally interpolated along the diagonal lines that connect points representing maximum and minimum absorbed energy for yield and failure points. For notation purposes, the stress-strain curves determined in this way were assigned a value K defined in equation (2) that corresponds to the deviation of yield and failure points from the average curve along the diagonal lines (Fig. 8).

$$K=(\sigma_u-\sigma_{u\,ave})/(\sigma_{u\,max}-\sigma_{u\,ave}) \qquad (2)$$

RESULTS

ESTIMATION OF IMPACT CONDITIONS

Table 1 summarizes the minimum values of the objective function and the corresponding design variables for both the S-4 and S-5 stances obtained from the MADYMO optimization. Fig. 9 shows the time histories of pedestrian kinematics obtained using the optimized design variables for each stance. These results were used as the impact conditions for injury prediction using the FE model.

INJURY PREDICTION USING FE MODEL

A parametric study was conducted using different bone stress-strain curves described above. For the S-4 stance, left tibia mid-shaft fracture sustained in the accident was predicted with the bone stress-strain curves corresponding to K between –0.63 and -0.82 (Fig. 10). For the S-5 stance, only left femur fracture was predicted with K between -0.5 and -0.74 (Fig. 11), and both left femur and tibia fractures were predicted with those at -0.75 or lower. Use of the S-5 stance did not yield the exact lower limb fracture sustained in the accident with any stress-strain curves.

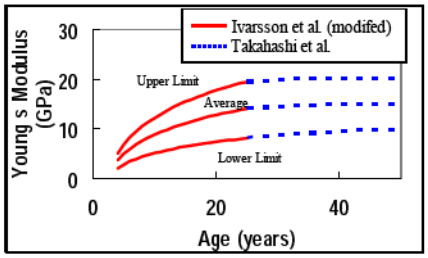

Fig. 6 Bone material property as a function of age (Femur Young's modulus)

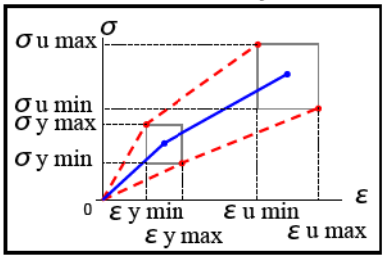

Fig. 7 Stress-Strain curves representing individual variation

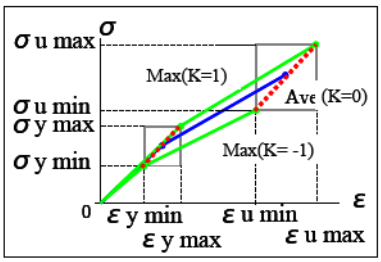

Fig. 8 Stress-Strain curves at maximum and minimum absorbed energy

Posture	Objcetive Funtion (m)	Vehicle Speed	Pedestrian Location (m)	Pedestrian Speed (m/s)
S-4	0.146	10.142	-0.324	2.931
S-5	0.104	12.111	-0.200	3.000

Table 1 Minimized objective function and design variables

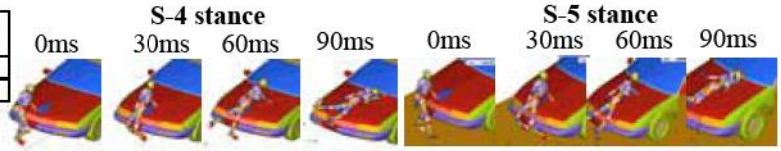

Fig. 9 Time history of pedestrian kinematics

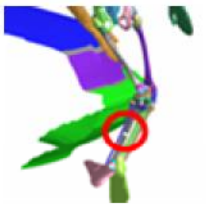

Fig. 10 Predicted lower limb injury for S-4 stance (material property：K=-0.63)

Fig. 11 Predicted lower limb injury for S-5 stance (material property：K=-0.5)

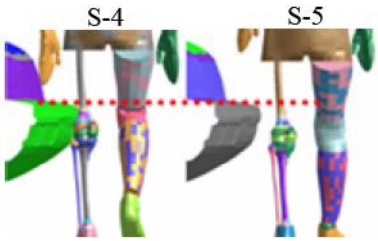

Fig. 12 Difference in bumper contact location between S-4 and S-5 stances

DISCUSSION AND CONCLUSION

Since the bumper stiffness was taken from a different vehicle, additional MADYMO and FE simulations were run. The results showed that the stiffness change by 10% had negligible effect on both overall kinematics and lower limb injury prediction for both the S-4 and S-5 stances.

The results of the lower limb injury prediction using the FE model for the S-4 and S-5 stances based on the impact conditions determined from the MADYMO optimization indicated that it was possible to reproduce injuries sustained by the case pedestrian (left tibia mid-shaft fracture) with only the S-4 stance. On the other hand, the results of the MADYMO optimization showed lower value of the objective function for the S-5 stance (0.10386) compared to that for the S-4 stance (0.14550). The position of the tip of the bumper immediately before impact for the S-5 stance corresponded to the diaphysis of the femur (Fig. 12). The femur was therefore more likely to fracture in this stance than the S-4 stance, and the FE simulation consistently predicted femur fracture. Given this result, it was conjectured that the stance in the accident was closer to the S-4 stance. Possible explanation on this discrepancy is that it is difficult to accurately reproduce localized lower limb deformations using a simplified MADYMO contact algorithm. Another cause could be the lack of sufficient contact location information.

For the S-4 stance, the FE simulations succeeded in predicting the exact lower limb fracture pattern sustained by the case pedestrian with some of the stress-strain curves within the estimated range of individual variations. This suggests that the FE model with the estimated child bone material properties and their variations is potentially capable of accurately reproducing lower limb fractures seen in car-child pedestrian accidents. More cases need to be reconstructed for higher confidence in the estimated material properties and their individual variations.

REFERENCES

Ivarsson, B. J. et al.: Lateral Injury Criteria for the 6-Year-Old Pedestrian - Part II: Criteria for the Upper and Lower Extremities, SAE Paper Number 2004-01-1755 (2004)

Langhaar, H. L.: Dimensional Analysis and Theory Models, Wiley, 1951, 166p. (ISBN-13 978-0471516781)

Mizuno, Y.: Summary of IHRA Pedestrian Safety WG Activities (2003) - Proposed Test Methods to Evaluate Pedestrian Protection Afforded by Passenger Cars, 18th International Technical Conference on the Enhanced Safety of Vehicles Proceedings, Paper Number 580 (2003)

Okamoto, M. et al.: Development of Finite Element Model for Child Pedestrian Protection, 18th International Technical Conference on the Enhanced Safety of Vehicles Proceedings, Paper Number 151 (2003)

Takahashi, Y. et al.: Development and Validation of the Finite Element Model for the Human Lower Limb of Pedestrians, STAPP Car Crash Journal, Vol.44, Paper Number 2000-01-SC22, p.335-355 (2000)